Inorg. Chem. **2005**, *44*, 6431–6438

Chain Structures in Alkali Metal Borophosphates: Synthesis and Characterization of $K_3[BP_3O_9(OH)_3]$ and $Rb_3[B_2P_3O_{11}(OH)_2]$

Bastian Ewald,[†] Yurii Prots,[†] Prashanth Menezes,[†] Srinivasan Natarajan,[‡] Hui Zhang,[†] and RÜdiger Kniep*,[†]

Max-Planck-Institut für Chemische Physik fester Stoffe, Nöthnitzer Strasse 40, 01187 Dresden, Germany, and Framework Solids Laboratory, Solid State and Structural Chemistry Unit, Indian Institute of Science, Bangalore 560012, India

Received March 24, 2005

Two new alkali metal borophosphates, $K_3[BP_3O_9(OH)_3]$ and $Rb_3[B_2P_3O_{11}(OH)_2]$, were synthesized by applying solvothermal techniques using ethanol as solvent. The crystal structures were solved by means of single-crystal X-ray diffraction ($K_3[BP_3O_9(OH)_3]$, monoclinic, *C*2/*c* (No. 15), $a = 2454.6(8)$ pm, $b = 736.3(2)$ pm, $c = 1406.2(4)$ pm, $\beta = 118.35(2)°$, $Z = 8$; $Rb_3[B_2P_3O_{11}(OH)_2]$, monoclinic, $P2_1/c$ (No. 14), $a = 781.6(2)$ pm, $b = 667.3(2)$ pm, $c = 2424.8(5)$ pm, $\beta = 92.88(1)°$, $Z = 4$). Both crystal structures comprise borophosphate chain anions. While for the rubidium compound a loop-branched chain motif is found as common for most of the chain anions in alkali metal borophosphates, the crystal structure of the potassium phase comprises the first open-branched chain with the highest phosphate content found so far in this group of compounds. Both chain anions are closely related to known anhydrous or hydrated phases, and the structural relations are discussed in terms of how the presence of OH groups and hydrogen bonds as well as number, charge, and size of charge balancing cations influence the 3D structural arrangement. The anionic entities are classified in terms of general principles of structural systematics for borophosphates.

Introduction

Since the intensive research activities on borophosphates started roughly 10 years ago,[1] the number of borophosphates and metalloborophosphates has grown steadily. The crystal chemistry of these compounds with anionic partial structures mainly built from tetrahedral building units reveals a large structural variety, similar to that of silicates and alumosilicates.[2] As boron can also be 3-fold coordinated, trigonal planar building blocks are possible as well. The ratio of condensed borate and phosphate units in the anions (B:P) is varying between 6:1 and 1:4. In all those various structures, comprising many different structural motifs, P−O−P connections have not been observed within the borophosphate anions,[3,4] although existing in pure phosphates. Thus, borophosphate anions with B:P ratios lower than 1:4 have not been found and additional phosphate units remain isolated in the crystal structures. This avoidance of P−O−P connections reminds one of the situation in alumosilicates where Al−O−Al bonds in tetrahedral arrangements are avoided (Loewenstein rule),[5] and it indicates that such a rule could be valid in borophosphates as well. For borophosphates a possible explanation for the missing P−O−P bonds can be found in Paulings fourth rule, that, in a crystal containing different cations, those of high charge and low coordination number tend not to share polyhedron elements with one another.[6] This rule is in good agreement with the observation that phosphate groups are terminal for increased phosphate content and the dimensionality of borophosphate anions decreases and isolated phosphate groups appear.

If one focuses on alkali metal borophosphates, there are six different compounds known to date in the systems $M_2O-B_2O_3-P_2O_5(-H_2O)$ (M = Li, Na, K, Rb, Cs)[7−13] with B:P

* To whom correspondence should be addressed. E-mail: kniep@cpfs.mpg.de. Fax: +49 (0) 351 4646 3002.
† Max-Planck-Institut für Chemische Physik fester Stoffe.
‡ Indian Institute of Science.

(1) Kniep, R.; Gözel, G.; Eisenmann, B.; Röhr, C.; Asbrand, M.; Kizilyalli, M. *Angew. Chem.* **1994**, *706*, 791; *Angew. Chem., Int. Ed. Engl.* **1994**, *33*, 749.
(2) Liebau, F. *Structural Chemistry of Silicates*; Springer-Verlag: Berlin, Heidelberg, Germany, 1985.
(3) Ewald, B.; Kniep, R. Manuscript in preparation.
(4) Kniep, R.; Engelhardt, H.; Hauf, C. *Chem. Mater.* **1998**, *10*, 2930.
(5) Loewenstein, W. *Am. Mineral.* **1954**, *39*, 92.
(6) Pauling, L. *J. Am. Chem. Soc.* **1929**, *51*, 1010.

10.1021/ic050441p CCC: $30.25
Published on Web 08/02/2005

Table 1. Chain Anions Present in Alkali Metal Borophosphates, Sorted by Descending B:P Ratio (Light Gray Tetrahedral, BO_4; Dark Gray Tetrahedra, PO_4; Gray Spheres, B; White Spheres, OH; Black Spheres, O)

Compound / Ref.	B:P	Anionic polymers	Chain type
$K[B_6PO_{10}(OH)_4]$[7]	6:1	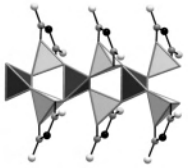	loop branched
$K_3[B_5PO_{10}(OH)_3]$[8]	5:1		loop branched
$Li[B_3PO_6(OH)_3]$[9]	3:1	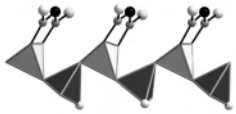	loop branched
$Na_5[B_2P_3O_{13}]$[10,11]	2:3		loop branched
$Rb_3[B_2P_3O_{11}(OH)_2]$ This work	2:3		loop branched
$K_3[BP_3O_9(OH)_3]$ This work	1:3	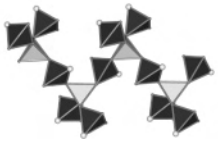	open branched

ratios ranging from 6:1 to 2:3 (Table 1). The dimensionality of the anionic partial structures in this group of borophosphates is predominantly that of a chain. Only two examples containing complex anions of higher dimensionality have been reported: The isotypic borophosphates $M^I[B_2P_2O_8(OH)]$ (M^I = Rb, Cs)[9] contain a 3D tetrahedral framework of alternating borate and phosphate units, and the structure of $Na_2[BP_2O_7(OH)]$[13] comprises a layered borophosphate partial structure. Borophosphate oligomers have not been observed up to now in this group of compounds. All known chains reveal three-membered ring motifs as they are common in the crystal structures of many borates.[14,15] The striking structural feature of the chains with high borate content (B:P = 6:1 to 3:1) is the presence of trigonal planar borate building units integrated in rings built exclusively of borate groups. While the crystal structures of $K[B_6PO_{10}(OH)_4]$[7] and $Li[B_3PO_6(OH)_3]$[9] contain borate loop-branches only, $K_3[B_5PO_{10}(OH)_3]$[8] comprises both, borate and phosphate loops. The phosphorus-rich chain borophosphate $Na_5[B_2P_3O_{13}]$ represents the only anhydrous alkali borophosphate and comprises a double-loop branched chain anion $^1_\infty[B_2P_3O_{13}^{5-}]$ with phosphate tetrahedra participating in the rings.[10,11] Unbranched chain motifs, as present in the crystal structures of $Fe[B_2P_2O_7(OH)_5]$[16] and $Al[B_2P_2O_7(OH)_5]\cdot H_2O$[17] (B:P = 1:1, vierer-single chain) or in the fluoride-substituted compound $(C_2H_{10}N_2)[BPO_4F_2]$ (B:P = 1:1, zweier-single chain),[18] have not been observed in the group of alkali metal borophosphates. Neither have open branched connection patterns, as known from other phosphate-rich borophosphates with B:P $\leq$ 2:3 (e.g. $M^{II}_3[BP_3O_{12}]$; M^{II} = Ba,[1] Pb[19]), been found in alkali metal compounds.

The number of borophosphates prepared by solid-state reactions or by using fluxes is rather small. Usually hydrothermal techniques are employed to obtain materials of high crystal quality. A comparatively new method utilizing alcohols in solvothermal experiments with boric and phosphoric acid has lately been reported for the synthesis of BPO_4 single crystals.[20] During the reactions in alcoholic media alkylated borate species are likely to be present, whereas the alkylation of phosphates is suppressed even by traces of water.[21,22] This is either present in the starting materials (85% H_3PO_4, nonpurified alcohols, crystal water) or a result of condensation reactions in the reaction vessel. Besides borate esters other components can be formed during the reactions as alcohols are known to decompose in the presence of phosphate catalysts.[23] The actual reaction mixture, the reaction conditions (pressure, pH, solubility), and the products formed are, thus, not only depending on the starting composition but also on the interaction of all participating chemical components. Changes in solvent polarity and the in-situ formation of alkylated precursor intermediates may give access to new phases such as the two new borophosphates, $K_3[BP_3O_9(OH)_3]$ and $Rb_3[B_2P_3O_{11}(OH)_2]$, reported here. Both title compounds comprise anionic chain entities with topologies that are known from related anhydrous borophosphates ($M^{II}_3[BP_3O_{12}]$; M^{II} = Ba,[1] Pb,[19] and $Na_5[B_2P_3O_{13}]$[10,11]). Structural similarities and differences of these structures are discussed in terms of the influence of cation size and charge as well as of the degree of protonation and the presence of hydrogen bonds. The crystal structure of $K_3[BP_3O_9(OH)_3]$ represents the first open-branched chain anion

(7) Boy, I.; Kniep, R. *Z. Naturforsch., B* **1999**, *54*, 895.
(8) Hauf, C.; Kniep, R. *Z. Kristallogr.*—New Cryst. Struct. **1996**, *211*, 707.
(9) Hauf, C.; Kniep, R. *Z. Kristallogr.*—New Cryst. Struct. **1996**, *212*, 313.
(10) Hauf, C.; Yilmaz, A.; Kizilyalli, M.; Kniep, R. *J. Solid State Chem.* **1998**, *140*, 154.
(11) Hauf, C.; Friedrich, T.; Kniep, R. *Z. Kristallogr.*—New Cryst. Struct. **1995**, *210*, 446.
(12) Hauf, C.; Kniep, R. *Z. Naturforsch., B* **1997**, *52*, 1432.
(13) Kniep, R.; Engelhardt, H. *Z. Anorg. Allg. Chem.* **1998**, *624*, 1291.
(14) Burns, P. C.; Grice, J. D.; Hawthorne, F. C. *Can. Mineral.* **1995**, *33*, 1131.
(15) Grice, J. D.; Burns, P. C.; Hawthorne, F. C. *Can. Mineral.* **1999**, *37*, 731.
(16) Boy, I.; Hauf, C.; Kniep, R. *Z. Naturforsch., B* **1998**, *42*, 631.
(17) Kniep, R.; Koch, D.; Borrmann, H. *Z. Kristallogr.*—New Cryst. Struct. **2002**, *217*, 187.
(18) Huang, Y. X.; Schäfer, G.; Borrmann, H.; Zhao, J. T.; Kniep, R. *Z. Anorg. Allg. Chem.* **2003**, *629*, 3.
(19) Park, C. H.; Bluhm, K. *Z. Naturforsch., B* **1995**, *50*, 1617.
(20) Schmidt, M.; Ewald, B.; Prots, Y.; Cardoso, R.; Armbrüster, M.; Loa, I.; Zhang, L.; Huang, Y.-X.; Schwarz, U.; Kniep, R. *Z. Anorg. Allg. Chem.* **2004**, *630*, 655.
(21) Cherbuliez, E.; Leber, J.-P. *Helv. Chim. Acta* **1952**, *35*, 644.
(22) Cherbuliez, E.; Leber, J.-P.; Ulrich, A.-M. *Helv. Chim. Acta* **1953**, *36*, 910.
(23) Moffat, J. B. *Catal. Rev.* **1978**, *18*, 199.

Table 2. Crystallographic Data and Refinement Parameters for $K_3[BP_3O_9(OH)_3]$ and $Rb_3[B_2P_3O_{11}(OH)_2]$[a]

param	$K_3[BP_3O_9(OH)_3]$	$Rb_3[B_2P_3O_{11}(OH)_2]$
fw	416.04	580.96
space group (No.)	*C*2/*c* (15)	$P2_1/c$ (14)
formula units	$Z = 8$	$Z = 4$
a, pm	2454.6(8)	781.6(2)
b, pm	736.3(2)	667.3(2)
c, pm	1406.2(4)	2424.8(5)
β, deg	118.35(2)	92.88(1)
V, nm^3	2.237(1)	1.2630(5)
calcd density, Mg/m^3	2.471	3.055
radiatn (λ, pm)	Mo Kα (71.073)	MoKα (71.073)
abs coeff, μ(Mo Kα), mm^{-1}	1.71	12.02
N(*hkl*) measd	16 356	12 734
N(*hkl*) unique	3818 ($R_{int} = 0.031$)	3523 ($R_{int} = 0.029$)
N(*hkl*) obsd [$I > 2\sigma(I)$]	3674	3021
refined params	181	199
final R indices [$I > 2\sigma(I)$]	R1 = 0.043	R1 = 0.029
	wR2 = 0.081	wR2 = 0.060
largest diff peaks, e·Å^{-3}	−0.55 and 0.54	−0.85 and 0.67

[a] The residuals are defined as follows: $R_{int} = \Sigma(F_o^2 - F_o^2(\text{mean}))/\Sigma(F_o^2)$; $R1 = \Sigma(|F_o| - |F_c|)/\Sigma|F_o|$; $wR2 = \{\Sigma[w(F_o^2 - F_c^2)^2/\Sigma[w(F_o^2)^2]\}^{1/2}$.

in the group of alkali borophosphates and has likewise the highest phosphate content (B:P = 1:3) observed so far. $Rb_3[B_2P_3O_{11}(OH)_2]$ represents the first rubidium borophosphate containing infinite chain anions.

Experimental Section

Syntheses. Both alkali metal borophosphates reported here were prepared solvothermally in Teflon-lined steel autoclaves ($V = 28$ mL) using ethanol as solvent with filling degrees of 30−40%. After a reaction time of typically 4 days, the autoclaves were removed from the furnace and allowed to cool to room temperature. The raw products were separated from the mother liquor by vacuum filtration. The transparent and colorless crystalline samples were washed with hot water, filtered, and washed again with acetone before they were dried in air at 333 K.

$K_3[BP_3O_9(OH)_3]$ was synthesized at $T = 493$ K from mixtures of 1.500 g (4.910 mmol) of $K_2B_4O_7{\cdot}4H_2O$ (Aldrich, ACS) and 8.018 g (58.920 mmol) of KH_2PO_4 (Merck, pa) according to a molar ratio of 1:12 (B:P = 1:3) that were homogenized by grinding before 1.132 g (9.820 mmol) of H_3PO_4 (85%, Merck, pa) was added.

$Rb_3[B_2P_3O_{11}(OH)_2]$ was prepared at $T = 443$ K from mixtures of 3.315 g (32.35 mmol) of RbOH (Aldrich), 1.000 g (16.17 mmol) of H_3BO_3 (Roth, 99%), and 3.729 g (32.35 mmol) of H_3PO_4 (85%, Merck, pa) according to a molar ratio of 2:1:2 which were homogenized before the reaction.

X-ray Powder Diffraction. X-ray powder investigations were performed with Cu Kα_1 radiation ($\lambda = 154.060$ pm) on a Huber G670 image plate camera with Guinier geometry. Intensity data were recorded up to 100° (2θ) and averaged from multiple measurements (6 × 30 min). X-powder diffraction data did not evidence any crystalline impurities for both compounds. The lattice parameters of $K_3[BP_3O_9(OH)_3]$ and $Rb_3[B_2P_3O_{11}(OH)_2]$ were refined with LaB_6 as internal standard ($a = 415.69$ pm).[24] The results based on 120 reflections between $8° < 2\theta < 84°$ for $K_3[BP_3O_9(OH)_3]$ and 152 reflections between $15° < 2\theta < 97°$ for $Rb_3[B_2P_3O_{11}(OH)_2]$ are given in Table 2 together with other relevant data of the single-crystal structure determinations.

Single-Crystal Structure Determination. Colorless single crystals of $K_3[BP_3O_9(OH)_3]$ (monoclinic prism, 0.050 × 0.050 × 0.150 mm^3) and $Rb_3[B_2P_3O_{11}(OH)_2]$ (monoclinic prism, 0.090 × 0.090 × 0.200 mm^3) were selected optically by means of homogeneous extinction of polarized light under an optical microscope and mounted on a glass fiber with two component epoxy resin.

X-ray intensity data for $K_3[BP_3O_9(OH)_3]$ with an index range of $-32 \le h \le 36$, $-8 \le k \le 10$, and $-20 \le l \le 20$ ($6° \le 2\theta \le 64°$) were collected on a Weissenberg type diffractometer (Rigaku R-Axis Rapid) with a curved imaging plate detector (radius $R = 127.4$ mm) and a 3-circle goniometer. Reflection intensities were corrected for absorption (multiscan routine, $R_{int} = 0.031$). The exctinction conditions *hkl*, $h + k = 2n$, and *h*0*l*, *h*, $l = 2n$, led to *C*2/*c* and *Cc* as possible space groups of which the centrosymmetric *C*2/*c* (No. 15) was found to be correct during the refinement. The crystal structure was solved by direct methods and refined by a full-matrix least-squares procedure.[25] The positions of the hydrogen atoms could be located in the difference Fourier maps (close to O1, O3, and O5), and their coordinates were refined as free variables. For the final anisotropic refinement steps the isotropic displacement parameters of the hydrogen atoms were restrained to $1.2U_{iso}$(O). A summary of the crystallographic data and refinement parameters is given in Table 2; the final atomic coordinates are listed in Table 3.

Table 3. Atomic Coordinates and Displacement Parameters (pm^2 × 10^{-1}) for $K_3[BP_3O_9(OH)_3]$ (Standard Deviations in Parentheses)

atom	*x*	*y*	*z*	U_{eq}/U_{iso}[a]
K1	0.2697(1)	−0.0007(1)	0.0877(1)	19(1)
K2	0.0543(1)	0.0725(1)	0.6593(1)	22(1)
K3	0.3912(1)	0.1672(1)	0.5226(1)	22(1)
B1	0.1668(1)	0.2692(3)	0.1556(2)	10(1)
P1	0.2421(1)	−0.0209(1)	0.8109(1)	11(1)
P2	0.1039(1)	0.1287(1)	0.9533(1)	11(1)
P3	0.4285(1)	0.0880(1)	0.8131(1)	12(1)
O1	0.4492(1)	0.0391(3)	0.4109(1)	21(1)
O2	0.0703(1)	−0.0063(2)	0.4914(1)	17(1)
O3	0.2046(1)	0.1326(3)	0.8282(2)	22(1)
O4	0.2653(1)	0.1573(2)	0.3992(1)	18(1)
O5	0.0555(1)	0.2406(3)	0.8548(1)	24(1)
O6	0.4839(1)	0.1993(3)	0.8226(1)	19(1)
O7	0.2022(1)	0.1000(2)	0.1955(1)	14(1)
O8	0.2951(1)	0.0700(2)	0.7965(1)	13(1)
O9	0.1436(1)	0.2775(2)	0.0383(1)	14(1)
O10	0.3827(1)	0.2343(2)	0.8145(1)	14(1)
O11	0.3967(1)	0.0164(3)	0.2082(1)	21(1)
O12	0.1460(1)	−0.0266(3)	0.4200(2)	26(1)
H11	0.4745(12)	0.0010(50)	0.4580(20)	25[b]
H31	0.1861(14)	0.0980(50)	0.8550(20)	27[b]
H51	0.0700(15)	0.3130(40)	0.8350(30)	29[b]

[a] U_{eq} is defined as one-third of the trace of the orthogonalized U_{ij} tensor. [b] U_{iso} values of the hydrogen atoms were held at $1.2U_{eq}$ of the oxygen atoms to which they are bound.

An individual crystal of $Rb_3[B_2P_3O_{11}(OH)_2]$ suitable for data collection was mounted on a Rigaku AFC7 diffractometer equipped with a Mercury CCD detector. Two measurements with long and short exposure times were performed to obtain accurate intensities of strong and weak reflections. Both data sets were combined and scaled using the program XPREP.[26] The resulting data set ($-10 \le h \le 10$, $-8 \le k \le 9$, $-33 \le l \le 25$; $5° \le 2\theta \le 60°$) was corrected for absorption using the multiscan procedure. Due to the nonambiguous extinction conditions *h*0*l*, $l = 2n$, and 0*k*0, $k = 2n$ (primitive monoclinic Bravais lattice), the crystal structure was solved in space

(24) *STOE Win XPOW*; Stoe & Cie GmbH: Darmstadt, Germany, 1999.

(25) *SHELXS-97/2: Program for the Solution of Crystal Structures and SHELXL-97/2: Program for Crystal Structure Refinement*; Universität Göttingen: Göttingen, Germany, 1997.

(26) *XPREP: Data Preparation & Reciprocal Space Exploration*, ver. 5.1 NT; Bruker Analytical Systems: Madison, WI, 1997.

Table 4. Atomic Coordinates and Displacement Parameters ($pm^2 \times 10^{-1}$) for $Rb_3[B_2P_3O_{11}(OH)_2]$ (Standard Deviations in Parentheses)

atom	*x*	*y*	*z*	U_{eq}/U_{iso}[a]
Rb1	0.5267(1)	0.2006(1)	0.3517(1)	27(1)
Rb2	0.7574(1)	0.2170(1)	0.1947(1)	33(1)
Rb3	0.8076(1)	0.2415(1)	0.0145(1)	23(1)
B1	0.1053(4)	0.3832(4)	0.1167(1)	15(1)
B2	0.1788(4)	0.0380(4)	0.1191(1)	14(1)
P1	0.0625(1)	0.2488(1)	0.3939(1)	11(1)
P2	0.2581(1)	0.2514(1)	0.2112(1)	16(1)
P3	0.3842(1)	0.2692(1)	0.0632(1)	15(1)
O1	0.1158(3)	0.1912(4)	0.2506(1)	32(1)
O2	0.4087(3)	0.2757(3)	0.0001(1)	24(1)
O3	0.0387(3)	0.0170(3)	0.3946(1)	24(1)
O4	0.1238(2)	0.8304(3)	0.1163(1)	18(1)
O5	0.1333(3)	0.3145(3)	0.4496(1)	24(1)
O6	0.1737(3)	0.3056(3)	0.3476(1)	23(1)
O7	0.1839(3)	0.4228(3)	0.1732(1)	22(1)
O8	0.2405(3)	0.4239(3)	0.0757(1)	19(1)
O9	0.2792(3)	0.0657(3)	0.1736(1)	21(1)
O10	0.3080(3)	0.0584(3)	0.0758(1)	18(1)
O11	0.0463(2)	0.1813(3)	0.1125(1)	15(1)
O12	0.4186(3)	0.3168(3)	0.2406(1)	26(1)
O13	0.5484(3)	0.3125(3)	0.0942(1)	22(1)
H11	0.131(7)	0.230(7)	0.281(2)	60(16)
H21	0.318(6)	0.244(6)	−0.017(2)	44(13)

[a] U_{eq} is defined as one-third of the trace of the orthogonalized U_{ij} tensor.

group $P2_1/c$ (No. 14). Initial atomic parameters were obtained from the interpretation of the maxima of Patterson functions, and the final model was determined from difference Fourier maps and refined by full-matrix least-squares methods.[25] The hydrogen atoms could be located in the difference Fourier maps close to O1 and O2. Atomic coordinates and isotropic displacement parameters of the hydrogen atoms were refined without restraints. Further crystallographic data and refinement parameters are summarized in Table 2; the final atomic parameters are given in Table 4.

Chemical Analyses. The elemental compositions of the reaction products obtained by solvothermal synthesis were investigated by means of inductively coupled plasma optical emission spectroscopy (ICP-OES) on a Varian Vista RL spectrometer with radial plasma observation. The results are averaged from three measurements of powdered samples dissolved in acids (HNO_3, HCl). The obtained compositions of K:B:P = 2.97(1):1.000(4):3.000(4) for $K_3[BP_3O_9(OH)_3]$ and Rb:B:P = 3.00(5):1.91(8):3.08(4) for $Rb_3[B_2P_3O_{11}(OH)_2]$ are in good agreement with the compositions of the single-crystal structure refinements, evidencing that pure products were yielded.

Thermal Analyses. Difference thermal analysis (DTA) and thermogravimetric measurements (TG) were performed using a Netzsch STA 409C simultaneous analyzer with Al_2O_3 crucibles and a type S thermocouple. The thermal stability was investigated between room temperature and 1373 K with heating/cooling rates of 10 K/min in dynamic argon atmosphere (gas flow 0.1 L/min). The argon gas (Messer-Griesheim, 99.999%) was additionally purified by passing over zeolite molecular sieves (Roth 3 Å, BTS-catalyst, Merck). All measurements are experimentally corrected for buoyancy.

Results and Discussion

$K_3[BP_3O_9(OH)_3]$: Crystal Structure and Characterization. The crystal structure of $K_3[BP_3O_9(OH)_3]$ contains complex anions $^1_\infty[BP_3O_9(OH)_3{}^{3-}]$ built of borate and monohydrogen phosphate tetrahedra linked via common vertexes. The B−O distances and O−B−O angles range from 146.0(3) to 146.9(3) pm and 107.2(2) to 113.0(2)°, respectively.

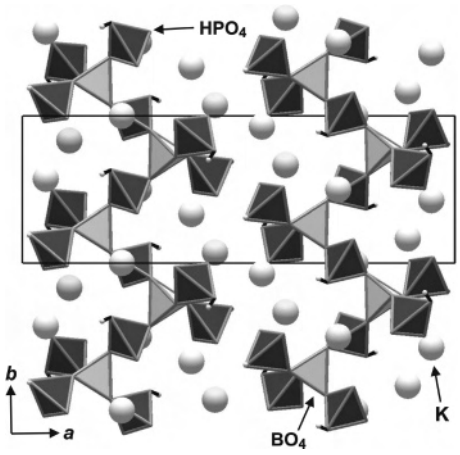

Figure 1. Open-branched vierer-single chains (B:P = 1:3) in the crystal structure of $K_3[BP_3O_9(OH)_3]$ (hydrogen atoms: small gray spheres). K^+ ions (big gray spheres) are located in the voids and intra- and interconnect the borophosphate strands in the crystal structure (8- and 9-fold coordinated by oxygen).

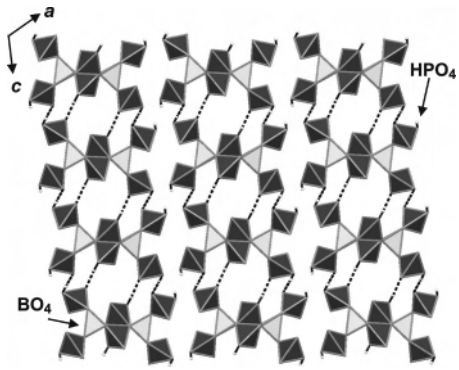

Figure 2. Open-branched chain anions $^1_\infty[BP_3O_9(OH)_3{}^{3-}]$ extending along [010] and interconnected via hydrogen bonds (dashed lines) to layers parallel to the *bc* plane.

In the hydrogen phosphate groups the P−O distances and O−P−O angles cover the ranges from 148.3(2) to 157.2(2) pm and 100.2(1) to 114.9(1)°, respectively. An infinite sequence of these tetrahedral units arranged in an alternating fashion forms the backbone of the chain. Additionally, the BO_4 tetrahedra share their two remaining vertexes with two branching monohydrogen phosphate groups. The anionic chains, in terms of silicate structural chemistry denoted as open-branched vierer-single chains,[2] are arranged parallel to [010] (Figure 1). Hydrogen bonds interconnect the chains to layers parallel to the *bc* plane (Figure 2). With short O−H distances of 75(2) and 76(2) pm and long O···H distances of 172(2) and 176(2) pm, the hydrogen bonds are clearly asymmetric and, as indicated by the O−H···O angles close to 180° (177(5) and 179(5)°), strongly directional.[27] Three distinct potassium sites are present in the crystal structure of $K_3[BP_3O_9(OH)_3]$, irregularly coordinated by eight and nine oxygen with K−O distances between 263.6(2) and 340.6(2) pm. The cations are placed in the voids of the chain structure, intra- and interconnecting the strands as shown in Figure 1.

The anionic partial structure of $K_3[BP_3O_9(OH)_3]$ reveals the same topology as the one of the anhydrous borophos-

(27) Steiner, T. *Angew. Chem.* **2002**, *114*, 56; *Angew. Chem., Int. Ed.* **2002**, *41*, 48.

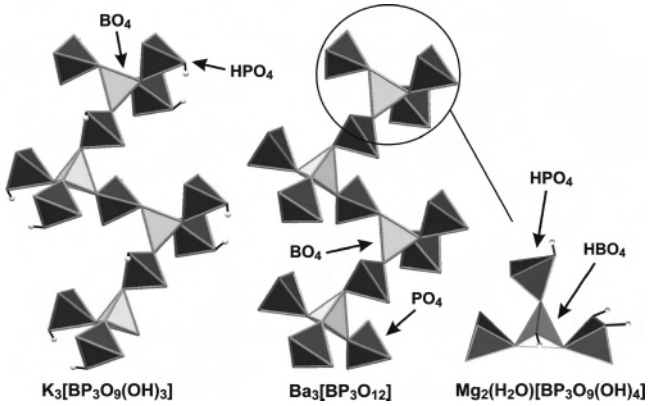

Figure 3. Crystal structures of $K_3[BP_3O_8(OH)_3]$ and $Ba_3[BP_3O_{12}]$[1] comprising topologically equivalent open-branched chain anions. These can be referred to a common fundamental building unit (FBU) (4□:[□]□|□|□|, right) which exists as isolated oligomer in the crystal structure of $Mg_2(H_2O)[BP_3O_9(OH)_4]$.[24] For further information, see the text.

phates $M^{II}_3[BP_3O_{12}]$ (M^{II} = Ba,[1] Pb[19]), which crystallize in the orthorhombic space groups *Ibca* (No. 73) and *Pbca* (No. 61), respectively. As illustrated in Figure 3, on disassembly of the chain anions a tetrameric fundamental building unit (FBU) can be defined,[14,15] which is known as isolated anion in the crystal structure of $Mg_2(H_2O)[BP_3O_9(OH)_4]$ (Figure 3, right).[28] To illustrate the FBU a structural descriptor can be used in which every tetrahedron is represented by a square symbol. Containing information about the number of participating tetrahedra (here: 4□) and the structural sequence (here: one central tetrahedron [□] connected to three adjacent ones □|□|□|), it has to be written as 4□:[□]□|□|□|.[14,15] The B:P ratio of 1:3 represents the highest possible phosphate content for chain structures due to the avoidance of P−O−P bonds. With B:P = 1:4 only borophosphate pentamers are found with one central borate unit connected to four phosphate groups such as present in $Pb_6[PO_4][B(PO_4)_4]$[29] and, protonated, in a templated polyoxomolybdenum borophosphate.[30]

The crystal structures of $K_3[BP_3O_9(OH)_3]$ and $Ba_3[BP_3O_{12}]$ show a very similar stacking of the tetrahedral chains (disregarding protons). The structural relationship can be illustrated with a simple 2D tiling model using projections along the *b* axis of $K_3[BP_3O_9(OH)_3]$ and along the *c* axis in the case of $Ba_3[BP_3O_{12}]$ (Figure 4). Two types of tiles (colorless and gray) are necessary to represent the chains in different orientations that are arranged in an alternating fashion. Starting from the higher symmetric anhydrous structure (Figure 4, top), the chains have just to be rotated around their 2-fold axes and slightly shifted along [010] to obtain the stacking found in the crystal structure of $K_3[BP_3O_9(OH)_3]$ (Figure 4, bottom). The differences are mainly due to the protonation and the presence of hydrogen bonds directing the chains. The ionic radii of K^+ and Ba^{2+} in 8-fold coordination have almost identical values (150−160 pm) and

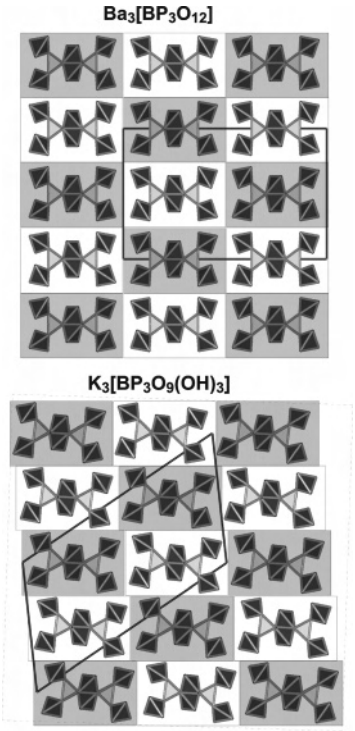

Figure 4. Comparative view on the crystal structures of $Ba_3[BP_3O_{12}]$[1] and $K_3[BP_3O_9(OH)_3]$: chain stacking described by a simple tiling model (protons omitted). Starting from the anhydrous compound $Ba_3[BP_3O_{12}]$, the chains just have to be slightly rotated and shifted to obtain the chain stacking as it is present in the title compound. For details, see the text.

Pb^{2+} is only slightly smaller (140−150 pm).[31,32] Therefore, the cations are placed on equivalent positions in the hydrated phase and the anhydrous phases (the structural comparison of $Ba_3[BP_3O_{12}]$ and $Pb_3[BP_3O_{12}]$ has been reported elsewhere).[19] The different orientation of the borophosphate chains, directed by the hydrogen bonds, leads to a lower symmetry in $K_3[BP_3O_9(OH)_3]$ (*C*2/*c*, No. 15) compared to the anhydrous structure of $Ba_3[BP_3O_{12}]$ (*Ibca*, No. 73, a = 2221.1 pm, b = 1429.6 pm, c = 710.2 pm).[1] This relationship can be described by a group−subgroup formalism[33,34] as illustrated in Figure 5. In the left part of the figure the translationengleiche symmetry reduction of index 2 (*t*2) and unit cell transformation is given; the relationship of the atomic coordinates of both structures is shown on the right. With the removal of the glide planes perpendicular to *a* and *c* in the space group *Ibca* all general positions 16*f* are split.

The investigations of the thermal stability of $K_3[BP_3O_9(OH)_3]$ revealed a one step mass loss of $\Delta m_{exp}/m = -6.5\%$ between 600 and 1000 K which matches the calculated loss of 1.5 mol of constitutional water per formula unit ($\Delta m_{calcd}/m = -6.5\%$). Complying with the weight loss, a strong endothermic peak is detected at T = 635 K (onset at T = 621 K). A small exothermic peak, detected at T = 912 K (onset at T = 876 K), remained unassigned. The sample molt

(28) Ewald, B.; Öztan, Y.; Prots, Y.; Kniep, R. *Z. Anorg. Allg. Chem.* **2005**, *631*, 1615.
(29) Belokoneva, E. L.; Ruchkina, O. V.; Dimitrova, O. V.; Stefanovich, S. Y. *Russ. J. Inorg. Chem.* **2001**, *46*, 179.
(30) Dumas, E.; Debiemme-Chouvy, C.; Sevov, S. C. *J. Am. Chem. Soc.* **2002**, *6*, 908.
(31) Shannon, R. D.; Prewitt, C. T. *Acta Crystallogr., Sect. B* **1969**, *25*, 925.
(32) Shannon, R. D.; Prewitt, C. T. *Acta Crystallogr., Sect. A* **1976**, *32*, 751.
(33) Bärnighausen, H. *Commun. Math. Chem.* **1980**, *9*, 139.
(34) Müller, U. *Z. Anorg. Allg. Chem.* **2004**, *630*, 1519.

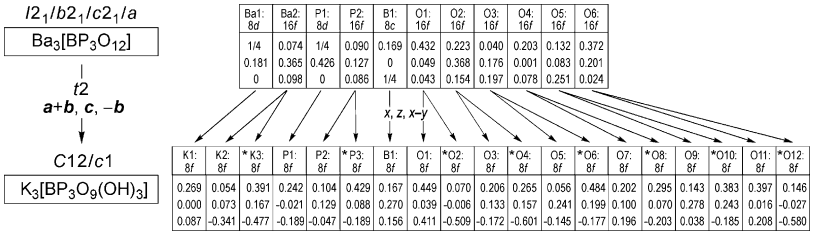

Ba1: 8d	Ba2: 16f	P1: 8d	P2: 16f	B1: 8c	O1: 16f	O2: 16f	O3: 16f	O4: 16f	O5: 16f	O6: 16f
1/4	0.074	1/4	0.090	0.169	0.432	0.223	0.040	0.203	0.132	0.372
0.181	0.365	0.426	0.127	0	0.049	0.368	0.176	0.001	0.083	0.201
0	0.098	0	0.086	1/4	0.043	0.154	0.197	0.078	0.251	0.024

K1: 8f	K2: 8f	*K3: 8f	P1: 8f	P2: 8f	*P3: 8f	B1: 8f	O1: 8f	*O2: 8f	O3: 8f	*O4: 8f	O5: 8f	*O6: 8f	O7: 8f	*O8: 8f	O9: 8f	*O10: 8f	O11: 8f	*O12: 8f
0.269	0.054	0.391	0.242	0.104	0.429	0.167	0.449	0.070	0.206	0.265	0.056	0.484	0.202	0.295	0.143	0.383	0.397	0.146
0.000	0.073	0.167	-0.021	0.129	0.088	0.270	0.039	-0.006	0.133	0.157	0.241	0.199	0.100	0.070	0.278	0.243	0.016	-0.027
0.087	-0.341	-0.477	-0.189	-0.047	-0.189	0.156	0.411	-0.509	-0.172	-0.601	-0.145	-0.177	0.196	-0.203	0.038	-0.185	0.208	-0.580

Figure 5. Group−subgroup relation[33,34] for the crystal structures of $Ba_3[BP_3O_{12}]$ (a = 2221.1 pm, b = 1429.6 pm, c = 710.2 pm)[1] and $K_3[BP_3O_{11}(OH)_3]$ (a = 2454.6(8) pm, b = 736.3(2) pm, c = 1406.2(4) pm, β = 118.35(2)°). Starting from the supergroup, the unit cell transformation and symmetry reduction ($t2$, translationengleiche of index 2) are given on the left. The relationship of atomic coordinates between the two structures is shown on the right. Positional parameters of the atoms generated by splitting are designated by an asterisk and correspond with those in $Ba_3[BP_3O_{12}]$ with the coordinates $-x + 1/2$, $y + 1/2$, z. The atomic positions of $K_3[BP_3O_{11}(OH)_3]$ correspond to those in Table 3 with the exception that for the z parameters $z + 1$ values are used.

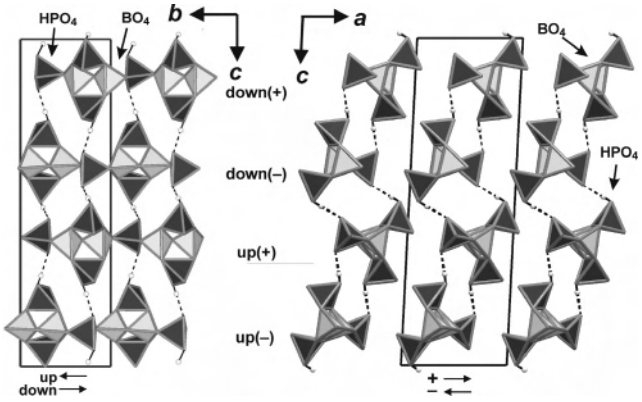

Figure 6. Loop-branched dreier-single chains in the crystal structure of $Rb_3[B_2P_3O_{11}(OH)_2]$ arranged parallel to [010] with opposite orientations (up and down as indicated by arrows). These are interconnected via hydrogen bonds (dashed lines) to corrugated layers parallel bc that are stacked at a distance of $a/2$ (right). Directed by hydrogen bonds, neighboring chains have different orientations in the layers which are indicated as + and − (right). Thus, chains alternate layerwise with the sequence down(+)−down(−)−up(+)−up(−). Hydrogen atoms are represented by gray spheres.

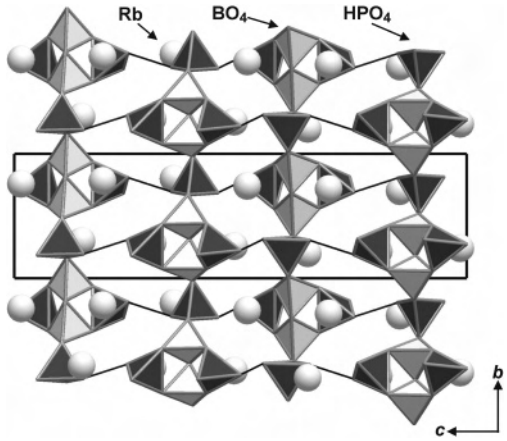

Figure 7. Cation positions in the crystal structure of $Rb_3[B_2P_3O_{11}(OH)_2]$: 8- and 9-fold coordinated Rb atoms are located between the layers of hydrogen-bonded borophosphate chains. In the view along [100] they are located above and below the layer (hydrogen bonds simplified as black lines, protons omitted).

during the experiment, the resolidified glassy residue is amorphous in terms of X-ray powder diffraction.

$Rb_3[B_2P_3O_{11}(OH)_2]$: Crystal Structure and Characterization. The crystal structure of $Rb_3[B_2P_3O_{11}(OH)_2]$ reveals a 1D infinite anionic arrangement of distorted borate and (hydrogen) phosphate tetrahedra that are linked via common corners. The B−O distances and O−B−O angles are varying from 141.3(4) to 151.4(4) pm and 105.2(2) to 115.3(2)°, respectively. For the phosphate groups P−O distances and O−P−O angles are found in a range 147.8(2)−156.6(6) pm and 103.7(1)−113.5(1)°, respectively. The backbone of the chain anions is built from tetrahedra alternating with a sequence of two borate tetrahedra followed by a phosphate unit. The two adjacent borate groups additionally share their remaining corners with two loop branching hydrogen phosphate groups, and the resulting structural motif is denoted as a double-loop-branched tetrahedral chain (Figure 6). These are arranged parallel to [010] and have opposite directions with respect to the b-axis (looking at the orientation of the polyhedra) which are defined as up and down (Figure 6, left, directions indicated). Adjacent chains are interconnected via hydrogen bonds to corrugated layers parallel to bc (Figure 6, right). The hydrogen bonds are strongly directional with O−H···O angles close to 180° (177(5) and 178(5)°). Short O−H (78(5) and 84(5) pm) and long O···H distances (166(5) and 171(5) pm) show that the bonds are clearly asymmetric.[27] The view along the chains (Figure 6, right) shows that directed by the hydrogen bonds neighboring chains have opposite orientations in the layer. The direction is indicated as + and − depending on the side to which the two phosphate branches point with respect to the a-axis. In each of the layers chains alternate with the sequence down(+)− down(−)−up(+)−up(−). The layers are stacked with the distance a = 781.6(2) pm, in the layers adjacent chains are about 660 pm apart from each other. The three unique rubidium sites are irregularly coordinated by eight and nine oxygen in a distance range up to 355.3(3) pm and are placed in the voids of the structure intra- and interconnecting the borophosphate strands (Figure 7).

Chain anions with the same topology but nonprotonated are present in the crystal structure of $Na_5[B_2P_3O_{13}]$ ($P2_1$, No. 4, a = 671.1 pm, b = 1161.8 pm, c = 768.6 pm, β = 115.2°).[10,11] As shown in Figure 8, both chains are referred to a common fundamental building unit (FBU) which can be illustrated by a descriptor[14,15] as follows: 5□:⟨3□⟩=⟨3□⟩□ (five tetrahedra 5□ forming two three-membered rings sharing two common tetrahedra ⟨3□⟩=⟨3□⟩ and one attached tetrahedron □). The anionic chains in the crystal structures of $M^{II}(C_4H_{12}N_2)[B_2P_3O_{12}(OH)]$ (M^{II} = Co,[35,36] Zn[36]) can be referred to the same FBU, but the chain periodicity is

(35) Bontchev, R. P.; Jacobson, A. J. *Mater. Res. Bull.* **2002**, *37*, 1997.
(36) Schäfer, G.; Borrmann, H.; Kniep, R. *Z. Anorg. Allg. Chem.* **2001**, *627*, 61.

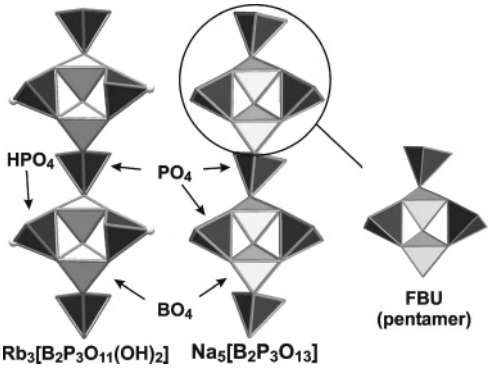

Figure 8. Crystal structures of $Rb_3[B_2P_3O_{11}(OH)_2]$ and $Na_5[B_2P_3O_{13}]$[10,11] comprising the same double loop-branched dreier-single chains in terms of topology. The anions can be disassembled to a common pentameric fundamental building unit (FBU, 5□:⟨3□⟩=⟨3□⟩□). For more details, see the text.

different due to conformational reasons. If the last unshared corner of the borate unit of this FBU is condensed to a phosphate group (forming a hexamer with B:P = 1:2), the units remain isolated like in the crystal structure of $Na_4Cu_3[B_2P_4O_{15}(OH)_2]\cdot 2HPO_4$[37] (P−O−P avoidance).

In a comparison of the crystal structures of $Rb_3[B_2P_3O_{11}(OH)_2]$ and $Na_5[B_2P_3O_{13}]$, both comprise the same double loop-branched dreier-single chain anions in terms of topology. The chemical differences, however, cause major differences in the structural arrangement. Besides the lower number of cations due to protonation of the complex anions in case of the Rb compound and the significant differences in cation sizes (8-fold coordination: $r(Na^+) \approx 125$ pm; $r(Rb^+) \approx 175$ pm),[31,32] hydrogen bonds influence the chain stacking and orientation. Nevertheless, the lattice parameters $a = 671.1(2)$ pm of the sodium compound and $b = 667.3(2)$ pm of $Rb_3[B_2P_3O_{11}(OH)_2]$ have almost identical values which comply with the translational period of the chain anions.

Chains with opposite orientation along [100] (defined as up and down) have to be regarded in case of the sodium compound which are stacked in layers in a distance of $b/2 = 581$ pm (Figure 9, top). In the layers each chain is 769 pm away from its nearest neighbor. In contrast to $Rb_3[B_2P_3O_{11}(OH)_2]$, all loop branches of the chains packed in a primitive motif are pointing in the same direction with respect to the *b*-axis as shown in the view along [100] (Figure 9, bottom). The sodium ions are found in the voids between the chains (Figure 10), and the additional cations (in comparison) are located in the direction where the hydrogen bonds are located in $Rb_3[B_2P_3O_{11}(OH)_2]$.

The differences of the structures are influenced by the number and size of the cations as well as by the hydrogen bonds. While the distances between the chains are predominantly defined by the ionic radii of the cations, the orientation of the chains is clearly controlled by the hydrogen bonds. The borophosphate chains appear to be very rigid as in both structures the chain lengths are almost identical and structural changes are just a result of the chain orientation.

(37) Boy, I.; Cordier, G.; Kniep, R. *Z. Kristallogr.*—New Cryst. Struct. **1998**, *213*, 29.

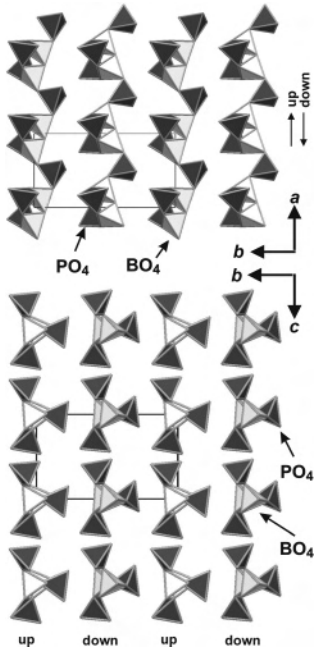

Figure 9. Anionic partial structure of $Na_5[B_2P_3O_{13}]$:[10,11] borophosphate chains are arranged parallel to [100] with two orientations (top, up and down, as indicated by arrows) organized layerwise. Layers with alternating orientation are stacked with a distance of $b/2 = 581$ pm (bottom). In the layers chains are 769 pm (complying with lattice parameter *a*) away from the nearest neighbors (with respect to the center). In contrast to $Rb_3[B_2P_3O_{11}(OH)_2]$ the chain packing motif is primitive and, if one looks along the chains (bottom), all loop branches are pointing in the same direction.

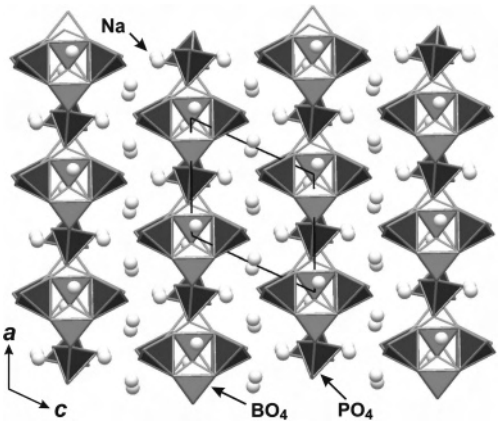

Figure 10. Location of sodium ions in $Na_5[B_2P_3O_{13}]$:[10,11] Na^+ ions are irregularly coordinated by oxygen and interconnect the borophosphate chains. The additional cations (in comparison) are placed in the direction where the hydrogen bonds (black lines in Figure 7) are located in $Rb_3[B_2P_3O_{11}(OH)_2]$.

On heating of samples of $Rb_3[B_2P_3O_{11}(OH)_2]$, a mass loss of $\Delta m_{exp}/m = -3.15\%$ is detected (between $T = 500$ K and $T = 750$ K), which is in good agreement with the value calculated for the release of one mole of constitutional water ($\Delta m_{calcd}/m = -3.10\%$). After the experiments, the samples are glassy and amorphous in terms of X-ray powder diffraction.

General Aspects. The solvothermal method proved to be a helpful and supplemental tool to synthesize new borophosphates as shown for $K_3[BP_3O_9(OH)_3]$ and $Rb_3[B_2P_3O_{11}(OH)_2]$. By using well-defined mixtures of alcohols and water it may be possible to "fine-tune" the polarity of the reaction

mixture and, thus, the solubility of potential products to access phases with a certain degree of protonation. The application of solvothermal techniques will be extended in the synthesis of borophosphates.

On thermal treatment, dehydration and glass formation is observed for both alkali metal borophosphates presented here. Starting from easy accessible crystalline phases, glasses of a distinct composition can be obtained. The properties of these glasses are currently under investigation.

It is evident from the known borophosphate structures that the B:P ratio influences the dimensionality of the anionic entities. Alkali metal borophosphates with high borate contents are only known with one-dimensional infinite (protonated) polymeric anions. With the decrease of B:P more and more B−O−P bonds are formed and, thus, the number of PO_4 branches increases until the borate groups share all oxygen with adjacent phosphate groups and open-branched motifs result. Layer and network structures are known with B:P = 1:1 and B:P = 1:2 only.[34] With B:P = 2:3 chain structures are found as well, e.g. in the crystal structures of $Na_5[B_2P_3O_{13}]$[10,11] and the new rubidium borophosphate presented here. Upon further increase of the phosphate content (B:P = 1:3) no higher dimensionality than that of a chain (e.g. in $K_3[BP_3O_9(OH)_3]$) has been observed. Due to the avoidance of P−O−P bonding the further decrease of B:P to 1:4 must necessarily reduce the dimensionality of the entity to that of an oligomer, as observed in $Pb_6[PO_4][B(PO_4)_4]$.[29] Future experiments will show the degree of this avoidance. The reason borophosphate partial structures of higher dimensionality have not been found for B:P > 1:1 remains so far unclear. A possible explanation is that the anions are predominantly protonated and do not contribute to interconnection.

To understand structure formation and appearance of certain connection patterns in borophosphate partial structures, structural systematics disassembling the anions into fundamental building units appear to be helpful.

Acknowledgment. We thank Dr. Rainer Niewa and Susann Müller for DTA/TG measurements as well as Dr. Gudrun Auffermann and Anja Völzke for chemical analyses.

Supporting Information Available: Crystallographic data in CIF format and TG plots of both compounds in PDF format. This material is available free of charge via the Internet at http://pubs.acs.org. The crystallographic data may also be obtained from the Fachinformationzentrum Karlsruhe, D-76344 Eggenstein-Leopoldshafen, Germany (fax, +49-7247-808-666; E-mail, crysdata@fiz-karlsruhe.de), by quoting the name of the author, the citation of the paper, and the depository numbers CSD-415664 for $K_3[BP_3O_9(OH)_3]$ and CSD-415665 for $Rb_3[B_2P_3O_{11}(OH)_2]$.

IC050441P